RESEARCH ARTICLE doi.org/10.1002/adsc.202500075 ADVANCED SYNTHESIS & CATALYSIS

Gram-Scale Photocatalysis with a Stable and Recyclable Chromium(III) Photocatalyst in Acetonitrile and in Water

Steven Sittel,[a] Julian Neuner,[a] Jonas M. Grenz,[a] Christoph Förster,[a] Robert Naumann,[a,*] and Katja Heinze[a,*]

[a] Department of Chemistry
Johannes Gutenberg University Mainz
Duesbergweg 10–14, 55128 Mainz (Germany)
E-mail: rnaumann@uni-mainz.de; katja.heinze@uni-mainz.de

Manuscript received: January 21, 2025; Revised manuscript received: March 12, 2025;
Version of record online: April 10, 2025

Supporting information for this article is available on the WWW under https://doi.org/10.1002/adsc.202500075

Abstract: The use of stable photosensitizers made on a multigram-scale from cheap and available starting materials offers an extraordinary opportunity to translate small-scale proof-of-concept photoreactions to widespread applications in non-specialized laboratories, thereby promoting the implementation of light-driven syntheses. Herein, we report an easy, multigram-scale preparation of the exceptionally photo- and redoxstable chromium(III) complex $\mathbf{[Cr(tpe)_2]^{3+}}$ (tpe = 1,1,1-tris(pyrid-2-yl)ethane) at room temperature. This photocatalyst was successfully employed in acetonitrile and in the "green" solvent water as demonstrated in visible-light induced Schenck-Ene reactions, Newman-Kwart rearrangements, radical cation Diels-Alder cycloadditions, oxidative decarboxylation and trifluoromethylation reactions with excellent substrate conversions and high turnover numbers. Gram-scale photocatalytic reactions were conducted using a simple round-bottom flask as reaction vessel and irradiation with energy-efficient blue LEDs or even with sunlight. The stable photocatalyst was successfully recycled in up to 90–92% yields after the photoreactions.

Keywords: Chromium; Photocatalysis; Photoredox Catalysis; Recycling; Upscaling

Introduction

Homogeneous photocatalysis and in particular photoredox catalysis has augmented the chemist's toolbox by generating organic triplet molecules or organic radicals using visible light and a suitable photocatalyst (PC). These mild conditions open up unique mechanistic pathways that are not accessible thermally and hold the potential for more sustainable synthetic chemistry (Figure 1a/1b).[1–9] Efforts of many research groups all over world have provided a panoply of PCs with different key properties.[10] The applicability of a PC in a given photocatalytic reaction is determined by its chemical, optical and electrochemical properties (Figure 1c) such as solubility in a given solvent, stability under the applied conditions, maximum absorption wavelength (λ_{max}), molar absorption coefficient at the excitation wavelength (ε_{max}), excited state energy ($E_{0\text{-}0}$) and excited state lifetime (τ) as well as ground and excited state reduction or oxidation potentials $E_{\frac{1}{2}}$ and $^*E_{\frac{1}{2}}$).[10,11] For example, the excited state redox potential $^*E_{\frac{1}{2}}$ determines the scope of substrates that can be oxidized or reduced by the excited PC. Meanwhile, rationally designed new PCs (Figure 1d) span a large range of excited state redox potentials, which cover large substrate and reaction scopes.[2,10,12] While the wide range of excited state potentials and the resulting large substrate scopes highlight the potential and opportunities that photoredox catalysis holds, widespread application outside dedicated photochemistry research groups has not been achieved. Industrial use of photocatalysis is subject of

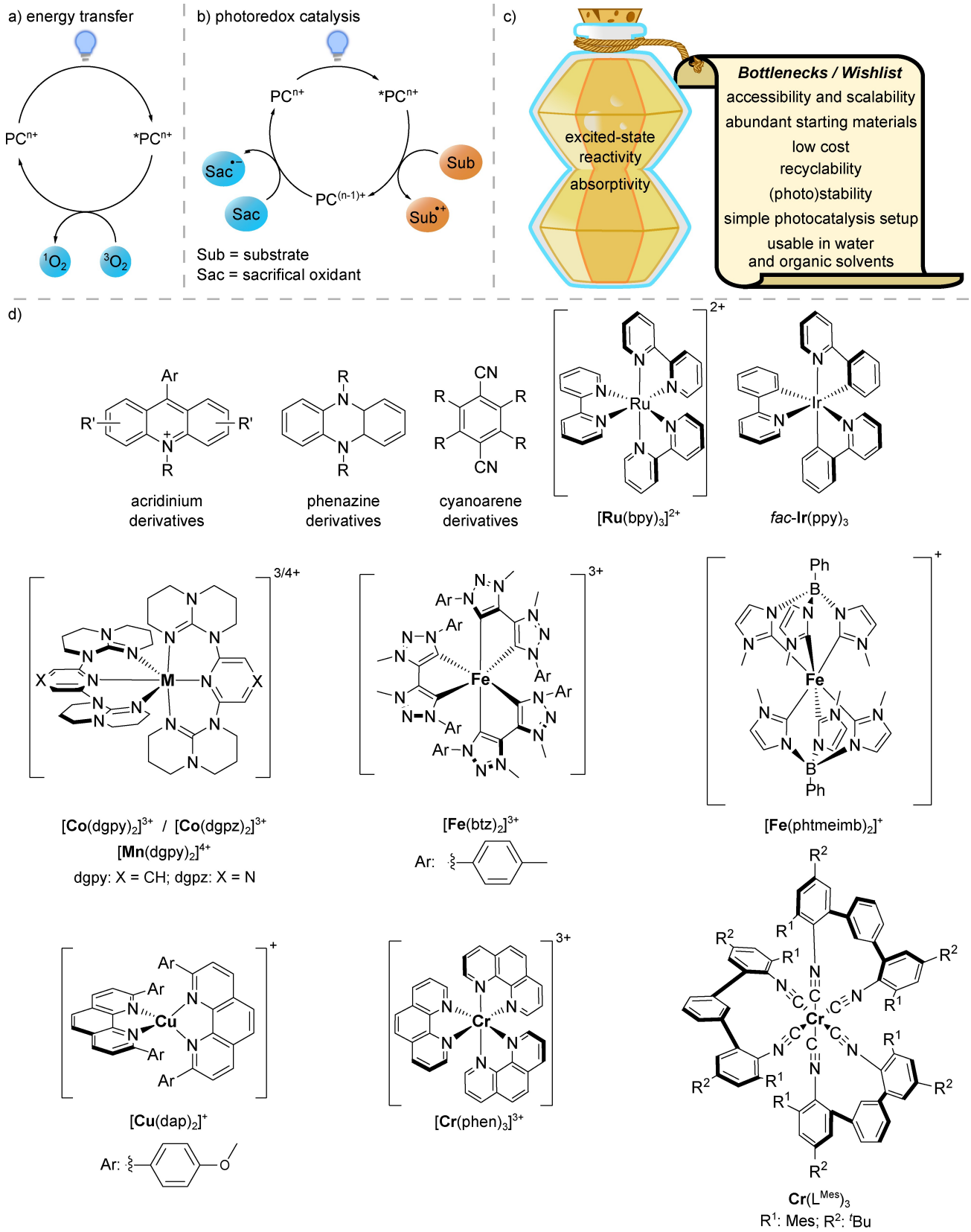

Figure 1. Schemes of a) energy transfer (to $^3O_2$) and b) photoredox catalysis with reductive quenching by a substrate Sub using a PC. c) Absorptivity and excited state reactivity are key aspects of PCs, yet the bottlenecks for widespread applications of photocatalysis beyond the cuvette or milligram-scale are often overlooked. d) Commonly employed organic and noble metal complex PCs and examples of earth-abundant metal complex PCs.

current research with respect to reactor design and scalability, in particular in the pharmaceutical and agrochemical sector.[13–16] Still, industrial and, perhaps even more strikingly, laboratory scale application of photoredox catalysis is very limited.[17–21] Given the impressive variety of PCs and photochemical transformations available, lack of reactivity or insufficient substrate scopes are not the main factors that prevent the use of photocatalysis in synthetic laboratories. Arguably, the most prevailing bottlenecks for photoredox catalytic transformations in synthetic laboratories are accessibility, cost, stability and recyclability of the PC, along with challenges in reactor design and the oftentimes low reaction quantum yield (Figure 1c). In the majority of the reported photocatalytic applications, complexes of noble transition metals, e.g. derivatives of $[Ru(bpy)_3]^{2+}$ or *fac*-$Ir(ppy)_3$ (Figure 1d, bpy = 2,2'-bipyridine; Hppy = 2-phenylpyridine), have been studied and employed as PCs, thanks to their strong visible light absorption, reversible redox chemistry, tunable ground and excited redox potentials and long lifetimes of the excited triplet metal-to-ligand charge transfer (^{3}MLCT) states.[2,10,11,22,23] However, the low abundance and hence high price of their central ions render these PCs inherently unsustainable and expensive.[24] Aiming to circumvent these drawbacks and to explore new reactivities, metal-free PCs have been developed more recently. These include strongly reducing phenazine derivatives and strongly oxidizing acridinium salts and cyanoarenes (Figure 1d).[10,23] However, these organic PCs often suffer from drawbacks, such as poor photostability or redox stability and limited solubility in the "green" solvent water.[12,25–28]

In addition to organic PCs, PCs containing earth-abundant metals have gained a lot of attention, comprising both strongly reducing and oxidizing complexes (Figure 1d).[10,29–31] Among the strongest photoreductants are arylisocyanide or carbonyl complexes of group VI metals. These possess long-lived ^{3}MLCT excited states and reach excited state potentials of up to $*E_{red} = -2.3$ V vs. SCE for $Cr(LMes)_3$ (Figure 1d).[32–34] Complexes of the $3d^{10}$ ion copper(I) have been employed in numerous photocatalytic transformations, exploiting their reducing ^{3}MLCT excited states (e.g. $[Cu(dap)_2]^+$; $*E_{red} = -1.43$ V vs. SCE; dap = 2,9-bis(p-anisyl)-1,10-phenanthroline).[29–31,35–37] Complexes with electron-poor metal centers possess oxidizing LMCT excited states which can achieve nanosecond excited state lifetimes.[29,38] The carbene iron(III) complexes $[Fe(btz)_3]^{3+}$ and $[Fe(phtmeimb)_2]^+$ ($*E_{red} = +1.9$ V and $+1.4$ V vs. SCE; btz = 3,3'-dimethyl-1,1'-bis(p-tolyl)-4,4'-bis(1,2,3-triazol-5-ylidene); phtmeimb$^-$ = tris(3-methylimidazolin-2-ylidene)(phenyl)borate, Figure 1d) absorb green light and engage in bimolecular reactions from their ^{2}LMCT states.[38–41] Photooxidants with cobalt(III) and manganese(IV) have been described (up to $*E_{red} = +2.75$ V and $+1.80$ V vs. SCE, Figure 1d), however their application in photocatalysis has remained very limited.[42–44] The LMCT excited state of the uranyl cation ($[U^{VI}O_2]^{2+}$ ($*E_{red} = +2.35$ V) is capable of oxidizing alkanes via hydrogen atom transfer under aerated conditions.[45–47] Chromium(III) complexes feature very long-lived doublet metal-centered excited states, so called spin-flip (SF) states.[48–50] These SF states can efficiently form singlet oxygen $^1O_2$ from $^3O_2$ regenerating the quartet ground state of the complex. This capability has been exploited for the photocatalyzed α-functionalization of aliphatic amines.[51,52] Although these SF states lack charge transfer character, they can be reductively quenched in bimolecular reactions,[31] which has been already exploited in various proof-of-concept photoredox catalytic reactions.[51,53–60] Some of these polypyridine chromium(III) complexes are even highly redox and photostable.[51,52] Despite these highly attractive chemical, photophysical and electrochemical properties,[31,48,50,61,62] chromium(III) complexes have thus far been underexplored in photo(redox) catalysis. In particular, large-scale reactions including PC recycling have not yet been reported.[51,53–59] Typically, the limited chemical and/or photostability of most homogeneous PCs causing them to degrade over the course of photochemical reactions, prohibits recycling of the PCs and effectively increases cost and decreases sustainability, due to the need for fresh material. Additionally, this instability of the PC potentially leads to contamination of the reaction product, necessitating more tedious purification steps and increasing waste production (e.g. solvents).

To make photocatalysis more attractive for the laboratory and industrial scale, an ideal PC should be easily accessible on a larger scale using only earth-abundant materials (accessibility and scalability). This PC should be chemically robust and photostable to allow simple and efficient product purification and PC recycling. Its optical absorption properties should be compatible with a simple reactor setup and its solubility should allow photocatalysis in organic solvents and in water.

In order to achieve these goals towards a sustainable and straightforward application of photocatalysis in non-specialized laboratories, we report the multigram-scale synthesis of a chromium(III)-based PC, probe its chemical robustness and photostability and apply this PC in exemplary energy transfer catalysis[63,64] providing $^1O_2$[65–68] and redox-neutral and oxidative photoredox catalysis[2,69] both in organic solvents and in water. We disclose upscaling of the photocatalysis with this PC to the multigram-scale using only common laboratory glassware, we demonstrate the use of sunlight instead of blue LEDs and we report the recycling of the PC.

Results and Discussion

Features of $[Cr(tpe)_2]^{3+}$

We selected the tricationic chromium(III) complex **$[Cr(tpe)_2]^{3+}$** (tpe = 1,1,1-tris(pyrid-2-yl)ethane) as a strongly photooxidizing, redox- and photostable PC.[51,56,70] The complex is highly soluble in acetonitrile or in water depending on the counter ion (see below). This PC features SF states at an energy $E_{0\text{-}0} = 1.75$ eV with an extremely long excited state lifetime of 3.5 ms in MeCN and 2.5 ms in H_2O recommending these SF states for efficient bimolecular quenching (Figure 2a; Figures S5 and S6). The complex is reduced at E_{red} ($[Cr]^{3+}/[Cr]^{2+}$) = −0.50 V vs. SCE in MeCN (Figure S12) resulting in an excited state reduction potential of $E_{red}(*[Cr]^{3+}/[Cr]^{2+}) = +1.25$ V vs. SCE in MeCN.[70] These values shift cathodically by about 0.2 V in water (Figure S13), yet the oxidative power of the SF states remain high so that many organic substrates are amenable to oxidation both in organic solvents and in water.

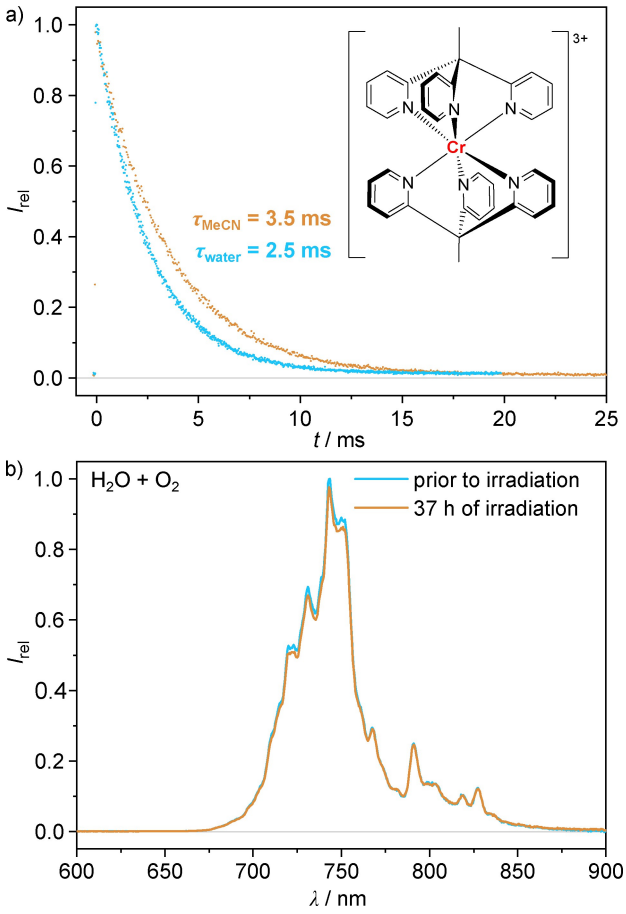

Figure 2. a) Emission decay traces of **$[Cr(tpe)_2]^{3+}$** in deaerated MeCN and in deaerated H_2O, recorded at 742 nm after excitation at 451 nm; structure of the complex cation **$[Cr(tpe)_2]^{3+}$**. b) Emission spectra of solutions of **$[Cr(tpe)_2][NO_3]_3$** in water under aerated conditions before and after irradiation at 460 nm using a 6.5 W UHP-LED for 37 h. Spectra are normalized to the emission maximum prior to irradiation.

The Cr complex absorbs blue light ($\lambda_{abs} = 431$ nm in MeCN; $\varepsilon_{431} = 35\ M^{-1}\ cm^{-1}$), allowing to use efficient blue LEDs for excitation (Figures S1 and S2).[71] The small molar absorption coefficient of **$[Cr(tpe)_2]^{3+}$** might seem counterintuitive for its application as PC,[10,22,72] in particular when considering that many traditional PCs possess strongly allowed transitions in the visible spectral region, such as $[Ru(bpy)_3]^{2+}$ with $\varepsilon_{452} = 13000\ M^{-1}\ cm^{-1}$.[11] However, very high molar absorption coefficients pose severe challenges for the design of efficient photoreactors. For example, if $[Ru(bpy)_3]^{2+}$ is used at a typical concentration of 2 mM, 99% of the incident light will be absorbed within the first 0.8 mm of the reaction solution according to the Beer-Lambert law (Figure S3).[73,74] Since the light cannot penetrate the solution any further, all $[Ru(bpy)_3]^{2+}$ molecules beyond this thin layer are catalytically inactive at any given moment, which is not a desirable scenario considering the high cost of precious metal PCs. The strong light absorption within the first few millimeters leads to local temperature spikes due to the high amount of energy absorbed per unit volume and to a high local concentration of organic radicals in a photoredox catalytic reaction. This can give rise to inhomogeneous kinetics within the photoreactor and to side reactions of the radicals. To circumvent these issues, flow reactors with very short optical path lengths have been receiving a lot of attention.[15,73,75–78] While the sophisticated design of these reactors is truly remarkable, these photoreactors are often expensive and poorly accessible for most laboratories, especially outside dedicated photochemistry research groups. In contrast, the most popular reaction vessels among chemists worldwide, like round-bottom flasks, are cheap and ubiquitous. Depending on their size, round-bottom flasks have optical path lengths of 5 to 15 cm or more. Assuming an optical path length of 10 cm, a 2 mM solution of **$[Cr(tpe)_2]^{3+}$** ($\varepsilon_{431} = 35\ M^{-1}\ cm^{-1}$) absorbs ca. 80% of the incident light over the entire length of the reactor (Figure S3). Despite the exponential nature of light attenuation, this leads to a comparably uniform distribution of photons throughout the reaction vessel, enlarging the photocatalytically active volume. Temperature spikes and side reactions are thus diminished. These properties recommend **$[Cr(tpe)_2]^{3+}$** as PC, especially in laboratory-scale reactions using standard glassware. Near quantitative absorption of the incident photons can be achieved by employing even longer path lengths or higher concentrations of **$[Cr(tpe)_2]^{3+}$**. While increasing the concentration of expensive noble-metal PCs, less stable PCs or PCs, which require tedious multistep syntheses,[32,33] is unsustainable, **$[Cr(tpe)_2]^{3+}$** can be employed in larger amounts due to its

simple, cheap and high-yielding preparation and its recyclability (see below). The photostability of **[Cr(tpe)$_2$]$^{3+}$** was probed by irradiating **[Cr(tpe)$_2$]$^{3+}$** in acetonitrile and water solutions with a UHP-LED (λ_{exc} = 460 nm, 6.5 W) under aerated and deaerated conditions. Negligible decomposition occurred after continuous irradiation over 25 to 42 h at this high photon intensity, according to the essentially unchanged photoluminescence spectra in all cases (Figure 2b; Figures S7–S9). Even under air, essentially no photodecomposition is noticeable despite the generation of $^1O_2$.[52] The O_2 and H_2O tolerance of **[Cr(tpe)$_2$]$^{3+}$** and ***[Cr(tpe)$_2$]$^{3+}$** (Figure 2b) is highly beneficial allowing a very simple experimental setup of the photocatalytic reaction under non-inert conditions. Hence, this chromium(III)-based PC is photostable in acetonitrile and in water, retains a millisecond excited state lifetime and a high excited state potential in both solvents and can be employed in standard laboratory glassware. Its optimized multigram-scale two-step preparation from commercially available starting materials will be discussed next.

Multigram-scale Preparation of the Photocatalyst [Cr(tpe)$_2$]$^{3+}$

The tridentate ligand tpe had been prepared by deprotonation of 2-ethylpyridine with *n*-butyllithium (*n*-BuLi) as a base in THF, followed by quenching with 2-fluoropyridine.[79–81] As the high reactivity and low selectivity of *n*-BuLi lead to side reactions at room temperature, cooling the reaction mixture with dry ice and dropwise addition of the *n*-BuLi solution are required. Both cooling and dropwise addition are energy-intensive and time-consuming for multigram-scale reactions involving large quantities of *n*-BuLi solutions. We hence replaced *n*-BuLi by lithium bis(trimethylsilyl)amide (LiHMDS) in refluxing THF in a one-pot synthesis (Figure 3a). On a 2 g-scale tpe was obtained in 85% yield. On a larger scale, spectroscopically pure tpe was obtained in 72%

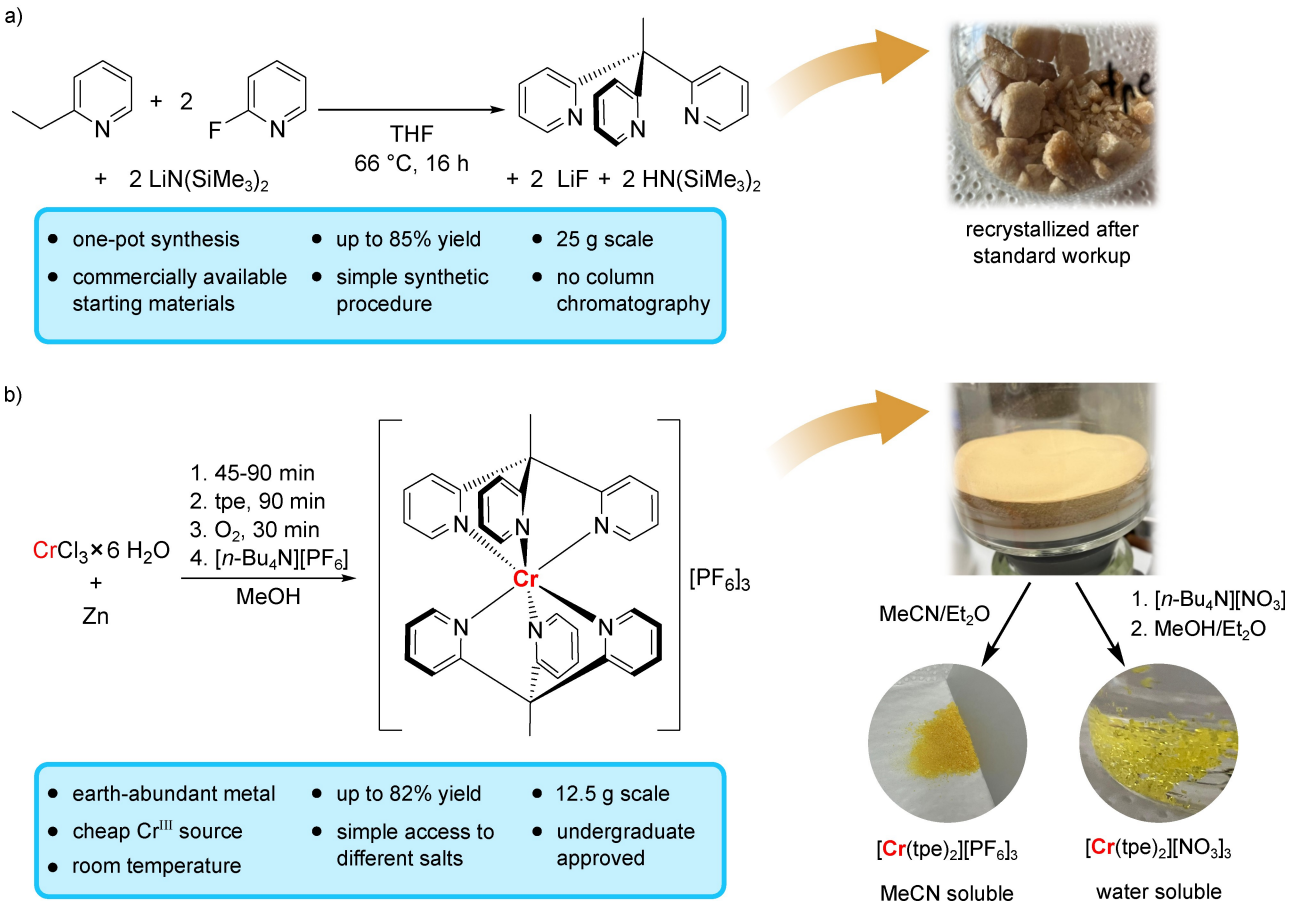

Figure 3. a) Synthesis of the tridentate ligand tpe. The photograph on the right-hand side shows 25.3 g of the ligand after standard workup and recrystallization from acetone. b) Synthesis of the PC **[Cr(tpe)$_2$]$^{3+}$** and access to its $[PF_6]^-$ and $[NO_3]^-$ salts. The photographs on the right-hand side show 12.5 g of the crude product after precipitation as $[PF_6]^-$ salt as well as the respective $[PF_6]^-$ and $[NO_3]^-$ salts after crystallization.

isolated yield (27.5 g; Figure S33, more details are given in the Supporting Information). Recrystallization from acetone gives highly pure tpe in 66% yield (25.3 g; Figure S34) without requiring further purification by column chromatography and thus reducing the amount of required solvent and produced waste.

Chromium(III) complexes are typically prepared from labile chromium(II) precursors.[82–85] **$[Cr(tpe)_2]^{3+}$** itself had been successfully prepared from anhydrous $CrCl_2$ as chromium source and the ligand tpe followed by air oxidation on a 0.5 g scale.[70] However, $CrCl_2$ is rather expensive and requires an inert atmosphere for long-term storage. Hence, we replaced $CrCl_2$ with the much cheaper and more accessible $CrCl_3 \times 6\ H_2O$ salt and used zinc as a cheap reductant to generate chromium(II) ions *in situ* (Figure 3b).[86] Addition of the thus prepared chromium(II) solution to a solution of tpe and subsequent air oxidation yields the target complex. This facile room-temperature synthesis route is high-yielding (up to 82%), scalable (confirmed up to 12.5 g) and lowers the material cost per mole (ca. 600 g) of **$[Cr(tpe)_2]^{3+}$** from ca. 4600 to ca. 2800 $ accounting for both the ligand and complex syntheses (for details of this estimation see the Supporting Information). On smaller scales (below 0.5 g $CrCl_3 \times 6\ H_2O$) the procedure can be further simplified to a one-pot reaction, by quickly adding the ligand solution to the chromium(II)/zinc mixture only slightly diminishing the yield to ca. 65%. Due to its simplicity and reliability, this procedure has even been integrated into an undergraduate laboratory course at our chemistry department paving the way for a broad application.

Depending on the choice of solvent in the photocatalytic reaction with the chromium(III)-based PC, **$[Cr(tpe)_2]^{3+}$** is isolated as the hexafluorophosphate salt **$[Cr(tpe)_2][PF_6]_3$** or the nitrate salt **$[Cr(tpe)_2][NO_3]_3$**, which are soluble in MeCN (ca. $10\ g\,L^{-1}$) and excellently soluble in water ($>100\ g\,L^{-1}$), respectively. The successful counterion exchange was confirmed by an XRD structure analysis of the $[NO_3]^-$ salt (Figure S14) and by infrared spectroscopy of both salts (Figures S15 and S16). Detailed procedures for the ligand and complex salt preparations are provided in the supporting information.

$[Cr(tpe)_2]^{3+}$ as Photosensitizer in Energy Transfer Catalysis and Photoredox Catalysis

A sustainable energy transfer catalysis requires a high stability of the PC in its ground and excited states under the reaction conditions and towards the generated excited substrates. For photoredox catalysis, a high stability of the reduced (or oxidized) intermediates is necessary in addition. Exemplary, we demonstrate the suitability of the chromium(III)-based PC in established reactions for both scenarios, namely for a light-sensitized energy transfer catalysis (Schenck-Ene reaction, Scheme 1a) and four redox-neutral and oxidative photoredox catalytic cycles, namely the Newman-Kwart rearrangement, the Diels-Alder cycloaddition, the photooxidative decarboxylation and the trifluoromethylation (Scheme 1b–e).

The ability to generate $^1O_2$ from the SF states of chromium(III) complexes is well-established.[51,52] Here we exemplary employ **$[Cr(tpe)_2]^{3+}$** as a photosensitizer in the type II oxygenation of an unactivated alkene (Schenck-Ene reaction).[67,68,87] The thus generated allylic hydroperoxides are useful precursors for the preparation of e. g. allylic alcohols, epoxy alcohols or unsaturated carbonyls.[68,88–91] Oleic acid as test substrate, **$[Cr(tpe)_2][PF_6]_3$** as photosensitizer in MeCN and blue light successfully leads to quantitative and clean conversion of the olefin to the corresponding hydroperoxides *trans*-9-hydroperoxyoctadec-10-enoic acid and *trans*-10-hydroperoxyoctadec-8-enoic acid in a 1:1 ratio (Scheme 1a)[92] as determined by ^1H NMR spectroscopy (Figure S36). The initial reaction quantum yield Φ_R was estimated at 0.1 (Figure S20). No conversion of the substrate occurred in the absence of **$[Cr(tpe)_2]^{3+}$**, O_2 or light (Figure S38).

As **$[Cr(tpe)_2]^{3+}$** is strongly oxidizing in its long-lived SF excited state both in MeCN and in H_2O, we exemplary discuss four photoredox catalytic applications using **$[Cr(tpe)_2]^{3+}$** in both solvents.

The Newman-Kwart rearrangement is a key step in the most important synthetic access to thiophenols from the corresponding phenols.[93–95] However, the originally described approach requires high reaction temperatures (200–300 °C) and electron-deficient arenes, limiting substrate scope and compromising selectivity and product purity. Alternative approaches to the Newman-Kwart rearrangement at less energy-demanding ambient temperature rely on the oxidative induction of the rearrangement by chemical oxidation,[96,97] electrochemical oxidation,[98] heterogenous photoredox catalysis,[99] homogenous photoredox catalysis with an organic pyrrylium PC and blue light,[100] and with 9,10-dicyanoanthracene using an osmium(II) complex sensitizer with red laser light via triplet-triplet annihilation upconversion.[101]

***$[Cr(tpe)_2]^{3+}$** should be thermodynamically competent to oxidize the phenol derivative *O*-(4-methoxyphenyl) dimethylcarbamo-thioate ($E_{red} = +1.1$ V vs. SCE; Scheme 1b) to initiate the rearrangement.[100] Indeed, a Stern-Volmer analysis confirmed the quenching of ***$[Cr(tpe)_2]^{3+}$** by the substrate ($k_q = 1.8\times10^5\ M^{-1}\ s^{-1}$; Figure S17).

Photocatalytic experiments confirmed that **$[Cr(tpe)_2]^{3+}$** is a suitable PC for this transformation in MeCN, resulting in >99% conversion to the rearranged product *S*-(4-methoxyphenyl) dimethylcarbamothioate (Figures S40 and S45). During the first 10 minutes of irradiation, an induction period is observed, which we attribute to photochemical oxida-

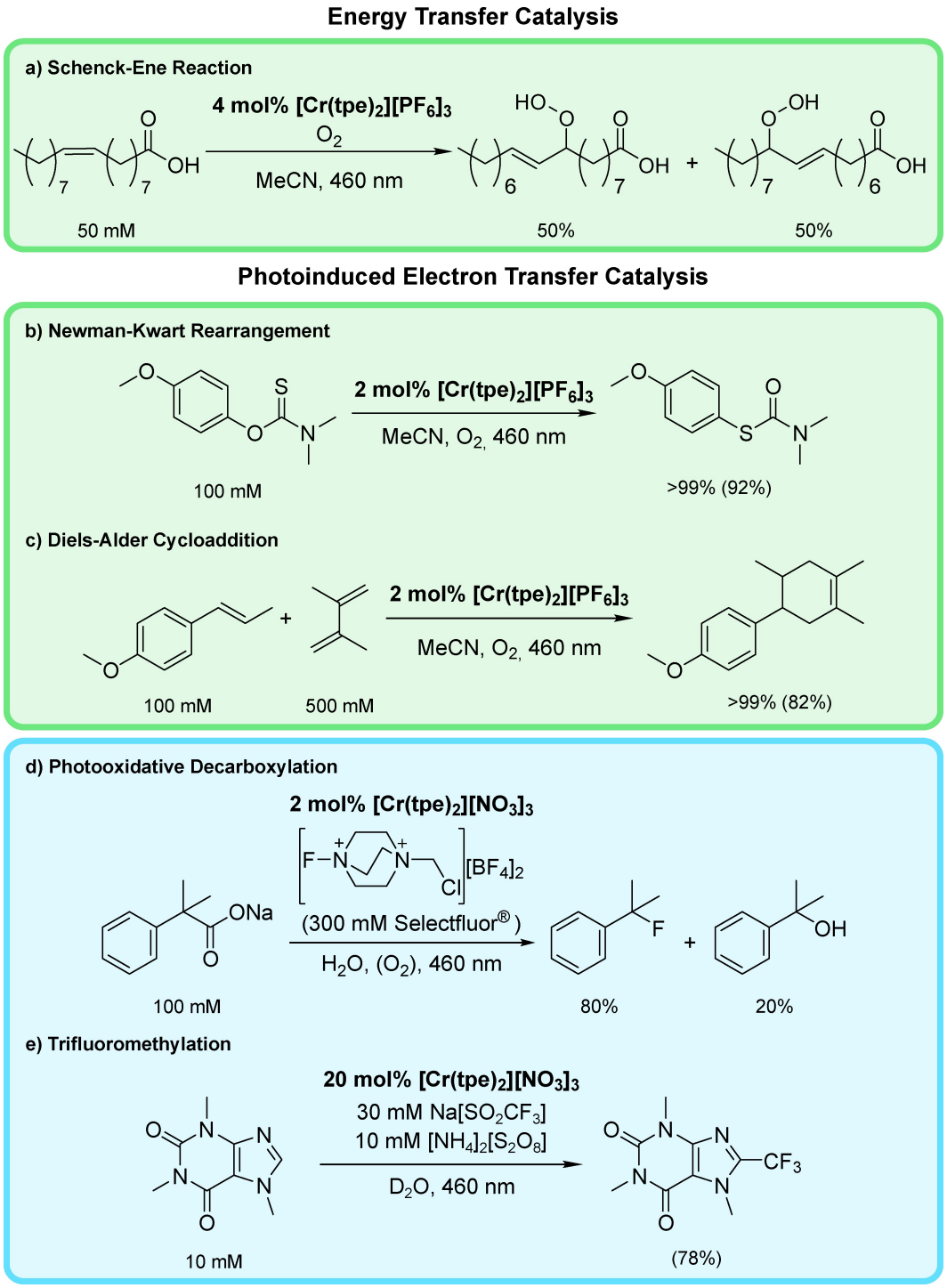

Scheme 1. Photocatalytic reactions catalyzed by $[Cr(tpe)_2]^{3+}$ in MeCN (green) and water (blue). Conversion of the starting material was determined via ^{1}H NMR spectroscopy. Isolated yields are given in parenthesis.

tion of trace impurities in the reaction mixture. After this induction period, the reaction proceeds with a high reaction quantum yield of $\Phi_R = 0.6$ (Figure S21). No conversion occurs in the absence of $[Cr(tpe)_2][PF_6]_3$ or light (Figure S44). Although the rearrangement is net redox-neutral, conducting the reaction in the presence of air accelerates the conversion (Figure S44). Likely, O_2 serves as redox mediator in this reaction, promoting the re-oxidation of the reduced PC and thus preventing detrimental charge recombination.[51] Hence, this photo-induced rearrangement is preferably performed simply under air, which obviates additional

sacrificial oxidants. This procedure was used to determine the achievable turnover number (TON) of the PC in this photocatalytic reaction. To this end, a MeCN solution of the PC (0.1 mM) and the substrate *O*-(4-methoxyphenyl) dimethylcarbamothioate (100 mM) was irradiated for 16 h. During this time, the substrate was fully converted to the product, corresponding to a TON of 1000 (Figure S41).

The visible light induced radical cation Diels-Alder cycloaddition[102] between *trans*-anethole and 2,3-dimethyl-1,3-butadiene using $\mathbf{[Cr(tpe)_2]^{3+}}$ as PC in MeCN on a small scale had been previously reported (Scheme 1c).[51] To estimate the TON for this reaction, a 0.1 mM MeCN solution of $\mathbf{[Cr(tpe)_2][PF_6]_3}$, containing 100 mM of *trans*-anethole and 500 mM of 2,3-dimethyl-1,3-butadiene was irradiated for 4.5 h achieving full conversion of *trans*-anethole to the cycloaddition product (Figure S48). As a chain-mechanism is involved in the cycloaddition mechanism,[103] the thus estimated TON = 1000 does not correspond to 1000 catalytic cycles of the PC. The unity quantum yield ($\Phi_R = 1$; Figure S22), which was estimated for the laboratory-scale experiments (discussed later in the manuscript), indicates that a chain mechanism indeed contributes to this transformation. These high numbers for both the light induced Newman-Kwart rearrangement and the radical cation Diels-Alder cycloaddition underline the high stability of $\mathbf{[Cr(tpe)_2]^{3+}}$ and the intermediates $\mathbf{*[Cr(tpe)_2]^{3+}}$ and $\mathbf{[Cr(tpe)_2]^{2+}}$ under the photocatalytic conditions. In real-world applications, a PC concentration as low as 0.1 mM would be suboptimal, as a lot of excitation light would be wasted. Hence, higher PC concentrations are preferred to accelerate the reactions, which is feasible due to the good availability of the PC (see above) and its recyclability (see below).

While acetonitrile is a popular solvent for many photocatalytic reactions and $\mathbf{[Cr(tpe)_2][PF_6]_3}$ is soluble and stable in MeCN, conducting photocatalysis in the "green" solvent water is especially desirable.[27] Yet, many PCs are insoluble in water or possess only short excited state lifetimes in water.[27,104,105] The easily accessible, water-soluble ($> 100\ g\,L^{-1}$) nitrate salt $\mathbf{[Cr(tpe)_2][NO_3]_3}$ solves these issues. Absorption and emission energies of the complex remain almost unchanged and the excited state lifetime is shortened by merely 30% to 2.5 ms (Figure S6). This is still an extremely long lifetime and bimolecular reactions in the excited state should be efficient even in water. The reduction potential of the $\mathbf{[Cr(tpe)_2]^{3+/2+}}$ half-reaction is shifted cathodically by merely 0.2 V (Figure S13), still allowing for oxidation of challenging substrates in the long-lived excited state.

Photocatalytic decarboxylative coupling reactions (e.g. Scheme 1d) have gained popularity, as they provide access to structurally diverse organic building blocks for the formation of challenging C–C and C–F bonds in Giese- and Hunsdiecker-type reactions, respectively.[106–108] While the classical approaches to these reactions typically suffer from the need for toxic additives and/or harsh reaction conditions, photocatalytic approaches have the potential to circumvent these issues.[109] Typical oxidation potentials of carboxylates lie around 1.3–1.7 V vs. SCE,[110] suggesting that their irreversible oxidation by $\mathbf{*[Cr(tpe)_2]^{3+}}$ in water is slightly uphill. In agreement with this thermodynamic estimation, the rate constant obtained from a Stern-Volmer quenching analysis of $\mathbf{[Cr(tpe)_2][NO_3]_3}$ with sodium 2-phenylisobutyrate in water is with $k_q = 5.9\times10^4\ M^{-1}s^{-1}$ rather small (Figure S18). We irradiated a solution of sodium 2-phenylisobutyrate with $\mathbf{[Cr(tpe)_2]^{3+}}$ as PC and Selectfluor®, which provides electrophilic fluorine as the coupling partner after the decarboxylation of the oxidized carboxylate.[111–113] Under aerated conditions, complete consumption of 2-phenylisobutyrate occurred (Figures S52 and S60). 2-Fluoro-2-phenylpropane and 2-phenyl-2-propanol were obtained in a 4:1 ratio according to ^{1}H NMR spectroscopy (Figures S55 and S56). Conducting the experiment under deaerated conditions yielded similar results, hence, working under air-free conditions is unneccesary. The alcohol by-product likely forms via oxidation of the generated cumyl radical to its carbocation and subsequent nucleophilic attack of water, similar to the reported interception of a benzyl cation by water yielding benzylalcohol.[114] Oxidation of the cumyl radical ($E_{red} = +0.16$ V vs. SCE)[115] under the reaction conditions either by Selectfluor® ($E_{red} = +0.33$ V vs. SCE)[116] or its oxidizing defluorinated derivatives $TEDA^+$ ($E_{red} = +0.79$ V vs. SCE)[117] or $TEDA^{2+\bullet}$ (no potential reported)[111,118] is thermodynamically feasible (TEDA = *N*-(chloromethyl)triethylenediamine; Figure S4). As oxygen is unnecessary to sustain photocatalysis, Selectfluor® or its derivatives can act as oxidants for the reduced photocatalyst $\mathbf{[Cr(tpe)_2]^{2+}}$.[119] Furthermore, $TEDA^{2+\bullet}$ has been reported as a chain carrier in various reactions.[111,118] Hence, it is conceivable that $TEDA^{2+}$ contributes to a chain mechanism in the present reaction as well. However, $\mathbf{[Cr(tpe)_2]^{3+}}$ as PC and light were necessary to induce the reaction (Figure S54). This demonstrates that $\mathbf{[Cr(tpe)_2][NO_3]_3}$ is a suitable PC in water, displaying sufficient oxidative power to oxidize an activated carboxylate. The reaction quantum yield was not determined for this transformation, as the oily products separate from the aqueous solution and the fluorinated product is volatile.

Similar to the photo-initiated oxidation of a carboxylate providing the carbon-centered radical after extrusion of CO_2, $\mathbf{*[Cr(tpe)_2]^{3+}}$ should be able to oxidize sulfinates, such as the bench-stable Langlois reagent sodium trifluoromethanesulfinate $Na[SO_2CF_3]$ delivering $^\bullet CF_3$ radicals after loss of SO_2.[120] Indeed,

$Na[SO_2CF_3]$ ($E_{red} = +1.02$ V vs. SCE)[121] quenches the emission of **$[Cr(tpe)_2][NO_3]_3$** in water with a quenching rate constant $k_q = 3.1\times10^5\ M^{-1}s^{-1}$ (Figure S19). Trifluoromethylated compounds are high-value products in the pharmaceutical and agrochemical sectors, as fluorine atoms strongly influence the biological activity of molecules. Mild and selective trifluoromethylation is therefore a hot topic and several synthetic pathways, including photoredox catalysis have been developed.[17,121–125] To test the applicability of **$[Cr(tpe)_2]^{3+}$** in light-activated trifluoromethylation and to demonstrate its tolerance towards highly reactive $^{\bullet}CF_3$ radicals, we employed **$[Cr(tpe)_2][NO_3]_3$** as PC in the trifluoromethylation of caffeine in water (Scheme 1e). D_2O was employed to facilitate reaction control by ^1H NMR spectroscopy. Irradiation of the reaction mixture under air resulted in a mixture of unidentified products. This likely results from the reaction of photogenerated $^{\bullet}CF_3$ radicals with oxygen, yielding highly reactive species, including fluorophosgene.[126] It was therefore necessary to exclude oxygen from the reaction mixture. As re-oxidation of **$[Cr(tpe)_2]^{2+}$** is very slow in the absence of an oxidant,[51] ammonium peroxodisulfate was added to the reaction mixture. Under these conditions, 78% of the caffeine substrate was transformed to the trifluoromethylated product 1,3,7-trimethyl-8-(trifluoromethyl)-7*H*-purine-2,6-dione after 4 h of irradiation (Figures S62 and S66). The reaction quantum yield was estimated at $\Phi_R = 0.004$ (Figure S23). In the absence of the PC, the product was detected in only 13% yield, while without ammonium peroxodisulfate or without light, no product forms (Figure S65). The successful photoredox catalyzed trifluoromethylation in water demonstrates the capability of **$[Cr(tpe)_2]^{3+}$** to operate in the presence of $^{\bullet}CF_3$ radicals, the strong ammonium peroxodisulfate oxidant and its highly reactive intermediates.[119,127,128] Furthermore, we have identified ammonium peroxodisulfate as cheap, water-soluble sacrificial oxidant, which serves as an alternative to molecular oxygen for the re-oxidation of **$[Cr(tpe)_2]^{2+}$**, when O_2 interferes with the organic reaction intermediates such as $^{\bullet}CF_3$ radicals.

Upscaling the Photocatalysis with $[Cr(tpe)_2]^{3+}$ and Recycling of the Photocatalyst

The Schenck-Ene reaction, the Newman-Kwart rearrangement and the radical cation Diels-Alder cycloaddition reactions were conducted on a gram-scale. Thanks to the low molar absorption coefficient of **$[Cr(tpe)_2]^{3+}$** making a longer path length beneficial, a round-bottom flask is in principle a suitable vessel for the irradiation of **$[Cr(tpe)_2]^{3+}$** as discussed above. Hence, 100 mL round-bottom flasks were used as reaction vessels. A blue UHP-LED as light source was placed next to the flask (Figure 4a). The non-purified

Figure 4. a) Photograph of the laboratory scale irradiation setup using a 100 mL round-bottom flask and a 460 nm UHP-LED. Intensity lowered to 5% to reduce overexposure on the photograph. b) Photograph of the irradiation setup using a 100 mL round-bottom flask and sunlight.

PC **$[Cr(tpe)_2][PF_6]_3$** was employed at a concentration of 2 mM in MeCN. This setup is very simple, cheap, quickly assembled and accessible in many chemical laboratories.

In the Schenck-Ene reaction 1.2 g oleic acid (50 mM substrate concentration) and the PC were irradiated in an open flask under vigorous stirring. This substrate was quantitatively and cleanly converted to the hydroperoxides within 4 h of irradiation with the UHP-LED according to NMR spectroscopy, while the hydroperoxides themselves were not isolated for safety reasons (Scheme 1a).

A quantitative Newman-Kwart rearrangement of the phenol derivative *O*-(4-methoxyphenyl) dimethylcarbamothioate was achieved using 1.7 g substrate (100 mM) within 60 min irradiation in the setup shown in Figure 4a (Scheme 1b). The pure thiophenol derivative was obtained after solvent evaporation and extraction of the residue with diethyl ether in 92% yield (1.55 g; Figure S40). Encouraged by the fast and quantitative photoreaction under these conditions, the Newman-Kwart rearrangement of *O*-(4-methoxyphenyl) dimethylcarbamothioate was also performed employing sunlight instead of the UHP-LED (Figure 4b). Full conversion of the substrate (20 mM) to the product was achieved after 8 h.

With the setup shown in Figure 4a, 1.2 g *trans*-anethole (100 mM, Figure S47) were quantitatively converted to the Diels-Alder cycloaddition product within 25 min of LED irradiation (Scheme 1c). The product was isolated after extraction with diethyl ether in 82% yield (1.52 g; Figure S49). Previously, this Diels-Alder cycloaddition had been performed with identical substrate concentrations, 1 mM of **$[Cr(tpe)_2]^{3+}$**, a shorter optical path length of ca. 1 cm and

a weaker excitation source (Aldrich® Micro Photochemical Reactor) requiring 6 h for completion.[51] This comparison underscores the importance of selecting a suitable light source and intensity, choosing optimal PC concentrations and optimizing the reactor setup and path length, when designing photochemical reactions to maximize the effective use of light as a reactant.

For all three photocatalytic gram-scale reactions, the PC was recovered after use. UV/vis spectroscopic analysis prior to and after the irradiation of the Newman-Kwart and Diels-Alder reaction mixtures indicated a high PC stability (Figures S28 and S29). After extraction of the respective organic products from the reaction mixtures, the remaining solid was dissolved in hot acetonitrile delivering spectroscopically clean and crystalline $\mathbf{[Cr(tpe)_2][PF_6]_3}$ after cooling and ether diffusion in 90–92% isolated yield (Figures S10 and S11). During the Schenck-Ene reaction, no significant catalyst decomposition was observed spectroscopically as well (Figure S27). To avoid isolating the hydroperoxide products, the PC was recovered from the reaction mixture in this case by adding [*n*-Bu_4N][NO_3], precipitating $\mathbf{[Cr(tpe)_2][NO_3]_3}$, which is less soluble in MeCN than the hexafluorophosphate salt. By this alternative procedure, 51% of the starting material was isolated. The only partial recovery results from incomplete precipitation of the nitrate salt in the presence of $[PF_6]^-$. The successful recycling of $\mathbf{[Cr(tpe)_2]^{3+}}$ as either $[NO_3]^-$ or $[PF_6]^-$ salt demonstrates the outstanding stability of the complex in photocatalytic applications and effectively lowers its cost and the amount of waste produced by reusing the same material and by avoiding laborious workup procedures.

Conclusion

This study demonstrates that the chromium(III) complex $\mathbf{[Cr(tpe)_2]^{3+}}$ with its exceptionally long excited state lifetime in the millisecond range can be successfully employed in photo(redox) catalytic applications in acetonitrile and in water. Its outstanding intrinsic photo- and redoxstability enables high turnover numbers and even the simple recovery of the intact photocatalyst after the photoreactions in high yields. This chromium(III)-based photocatalyst furnishes highly efficient Schenck-Ene reactions, photoinduced Newman-Kwart rearrangements and Diels-Alder cycloadditions in acetonitrile. The high photooxidative power of $\mathbf{[Cr(tpe)_2]^{3+}}$ even in water is exploited in the oxidation of an activated sodium carboxylate giving the decarboxylated fluorinated product with Selectfluor® as fluorine source. Analogously, photooxidation of sodium trifluoromethanesulfinate delivers $^{\bullet}CF_3$ radicals which add to caffeine as model substrate. Ammonium peroxodisulfate was identified as a suitable, cheap sacrificial oxidant for this oxygen sensitive reaction. Beyond small scale experiments, gram-scale photoreactions were demonstrated with this photocatalyst using simple, widely available round-bottom flasks and energy-efficient blue LEDs or even sunlight. The photocatalyst itself was prepared at room-temperature in quantities up to 12.5 g from cheap, commercially available starting materials in few reaction steps.

This study highlights a photo(redox) catalyst made from earth-abundant elements with highly desirable properties for widespread applications in synthetic laboratories, namely good accessibility, high stability in different oxidation states, recyclability, water solubility, applicability in various photoreaction types and utilization of a very simple experimental setup. This photocatalyst thus contributes to a more widespread translation of light-driven chemistry to synthetic laboratories and beyond.

Supporting Information

The Supporting Information contains experimental details, syntheses, optical and electrochemical characterization of the title complex, Stern-Volmer data, XRD data, IR spectra, ^1H and ^{19}F NMR spectra (PDF). A separate file (.zip) containing the original NMR data is provided in addition.

Acknowledgements

This work has been financially supported by the Deutsche Forschungsgemeinschaft (DFG) under grants INST 247/1018-1 and HE2778/10-2 and by the Top-Level Research Area SusInnoScience of Johannes Gutenberg University Mainz funded by the Research Initiative of the State of Rhineland-Palatinate (Germany). We thank Elena Meßmer and Nadine Gorzolka for preparative support. We thank Dr. Dieter Schollmeyer for collecting the XRD data. Open Access funding enabled and organized by Projekt DEAL.

References

[1] J. W. Tucker, C. R. J. Stephenson, *J. Org. Chem.* **2012**, *77*, 1617.
[2] M. H. Shaw, J. Twilton, D. W. C. MacMillan, *J. Org. Chem.* **2016**, *81*, 6898.
[3] F. Meyer, P. S. Halasyamani, G. Masson, *ACS Org. Inorg. Au* **2022**, *3*, 1.
[4] R. C. McAtee, E. J. McClain, C. R. J. Stephenson, *Trends Chem.* **2019**, *1*, 111.
[5] B. König, *Eur. J. Org. Chem.* **2017**, *2017*, 1979.
[6] A. Y. Chan, I. B. Perry, N. B. Bissonnette, B. F. Buksh, G. A. Edwards, L. I. Frye, O. L. Garry, M. N. Lavagnino, B. X. Li, Y. Liang, E. Mao, A. Millet, J. V. Oakley, N. L. Reed, H. A. Sakai, C. P. Seath, D. W. C. MacMillan, *Chem. Rev.* **2022**, *122*, 1485.

[7] L. Marzo, S. K. Pagire, O. Reiser, B. König, *Angew. Chem. Int. Ed.* **2018**, *57*, 10034.
[8] I. Ghosh, L. Marzo, A. Das, R. Shaikh, B. König, *Acc. Chem. Res.* **2016**, *49*, 1566.
[9] S. B. Cahoon, T. P. Yoon in *Free Radicals: Fundamentals and Applications in Organic Synthesis 1* (Hrsg.: L. Fensterbank, C. Ollivier), Georg Thieme Verlag KG, Stuttgart, **2021**.
[10] D. Kim, T. S. Teets, *Chem. Phys. Rev.* **2022**, *3*, 021302.
[11] D. M. Arias-Rotondo, J. K. McCusker, *Chem. Soc. Rev.* **2016**, *45*, 5803.
[12] N. A. Romero, D. A. Nicewicz, *Chem. Rev.* **2016**, *116*, 10075.
[13] E. E. Callard-Langdon, A. Steven, R. J. Kahan, *ChemCatChem* **2023**, *15*, e202300537.
[14] E. Kayahan, M. Jacobs, L. Braeken, L. C. Thomassen, S. Kuhn, T. van Gerven, M. E. Leblebici, *Beilstein J. Org. Chem.* **2020**, *16*, 2484.
[15] L. Buglioni, F. Raymenants, A. Slattery, S. D. A. Zondag, T. Noël, *Chem. Rev.* **2022**, *122*, 2752.
[16] N. C. Neyt, D. L. Riley, *React. Chem. Eng.* **2021**, *6*, 1295.
[17] J. W. Beatty, J. J. Douglas, K. P. Cole, C. R. J. Stephenson, *Nat. Commun.* **2015**, *6*, 7919.
[18] J. C. G. Kürschner, L. Brüss, L. Naesborg, *Chem. Eur. J.* **2023**, *29*, e202300627.
[19] P. Püllmann, D. Homann, T. A. Karl, B. König, M. J. Weissenborn, *Angew. Chem. Int. Ed.* **2023**, *62*, e202307897.
[20] Y.-M. Tian, W. Silva, R. M. Gschwind, B. König, *Science* **2024**, *383*, 750.
[21] K. P. Cole, J. J. Douglas, T. Hammerstad, C. R. J. Stephenson, *Org. Process Res. Dev.* **2023**, *27*, 399.
[22] D. Kim, V. Q. Dang, T. S. Teets, *Chem. Sci.* **2024**, *15*, 77.
[23] J. D. Bell, J. A. Murphy, *Chem. Soc. Rev.* **2021**, *50*, 9540.
[24] W. M. Haynes, D. R. Lide, T. J. Bruno, *CRC Handbook of Chemistry and Physics*, 97. Ed., CRC Press, **2016**.
[25] E. M. S. Stennett, M. A. Ciuba, M. Levitus, *Chem. Soc. Rev.* **2014**, *43*, 1057.
[26] A. P. Demchenko, *Methods Appl. Fluoresc.* **2020**, *8*, 22001.
[27] C. Russo, F. Brunelli, G. C. Tron, M. Giustiniano, *J. Org. Chem.* **2023**, *88*, 6284.
[28] S. Fukuzumi, K. Ohkubo, *Org. Biomol. Chem.* **2014**, *12*, 6059.
[29] C. B. Larsen, O. S. Wenger, *Chem. Eur. J.* **2018**, *24*, 2039.
[30] B. M. Hockin, C. Li, N. Robertson, E. Zysman-Colman, *Catal. Sci. Technol.* **2019**, *9*, 889.
[31] C. Förster, K. Heinze, *Chem. Phys. Rev.* **2022**, *3*, 41302.
[32] N. Sinha, C. Wegeberg, D. Häussinger, A. Prescimone, O. S. Wenger, *Nat. Chem.* **2023**, *15*, 1730.
[33] T. Jin, D. Wagner, O. S. Wenger, *Angew. Chem. Int. Ed.* **2024**, *63*, e202314475.
[34] W. R. Kitzmann, M.-S. Bertrams, P. Boden, A. C. Fischer, R. Klauer, J. Sutter, R. Naumann, C. Förster, G. Niedner-Schatteburg, N. H. Bings, J. Hunger, C. Kerzig, K. Heinze, *J. Am. Chem. Soc.* **2023**, *145*, 16597.
[35] Y. Zhang, Q. Wang, Z. Yan, D. Ma, Y. Zheng, *Beilstein J. Org. Chem.* **2021**, *17*, 2520.
[36] C. Sandoval-Pauker, G. Molina-Aguirre, B. Pinter, *Polyhedron* **2021**, *199*, 115105.
[37] M. Pirtsch, S. Paria, T. Matsuno, H. Isobe, O. Reiser, *Chem. Eur. J.* **2012**, *18*, 7336.
[38] L. H. M. de Groot, A. Ilic, J. Schwarz, K. Wärnmark, *J. Am. Chem. Soc.* **2023**, *146*, 9369.
[39] A. Ilic, J. Schwarz, C. Johnson, L. H. M. de Groot, S. Kaufhold, R. Lomoth, K. Wärnmark, *Chem. Sci.* **2022**, *13*, 9165.
[40] Y. J. Jang, H. An, S. Choi, J. Hong, S. H. Lee, K.-H. Ahn, Y. You, E. J. Kang, *Org. Lett.* **2022**, *24*, 4479.
[41] A. Aydogan, R. E. Bangle, A. Cadranel, M. D. Turlington, D. T. Conroy, E. Cauët, M. L. Singleton, G. J. Meyer, R. N. Sampaio, B. Elias, L. Troian-Gautier, *J. Am. Chem. Soc.* **2021**, *143*, 15661.
[42] A. K. Pal, C. Li, G. S. Hanan, E. Zysman-Colman, *Angew. Chem. Int. Ed.* **2018**, *57*, 8027.
[43] N. R. East, R. Naumann, C. Förster, C. Ramanan, G. Diezemann, K. Heinze, *Nat. Chem.* **2024**, *16*, 827.
[44] A. Y. Chan, A. Ghosh, J. T. Yarranton, J. Twilton, J. Jin, D. M. Arias-Rotondo, H. A. Sakai, J. K. McCusker, D. W. C. MacMillan, *Science* **2023**, *382*, 191.
[45] H. D. Burrows, T. J. Kemp, *Chem. Soc. Rev.* **1974**, *3*, 139.
[46] W.-D. Wang, A. Bakac, J. H. Espenson, *Inorg. Chem.* **1995**, *34*, 6034.
[47] L. Capaldo, D. Merli, M. Fagnoni, D. Ravelli, *ACS Catal.* **2019**, *9*, 3054.
[48] W. R. Kitzmann, J. Moll, K. Heinze, *Photochem. Photobiol. Sci.* **2022**, *21*, 1309.
[49] C. Förster, K. Heinze, *Adv. Inorg. Chem.* **2024**, p. 111–159.
[50] W. R. Kitzmann, K. Heinze, *Angew. Chem. Int. Ed.* **2023**, *62*, e202213207.
[51] S. Sittel, R. Naumann, K. Heinze, *Front. Chem.* **2022**, *10*, 887439.
[52] S. Otto, A. M. Nauth, E. Ermilov, N. Scholz, A. Friedrich, U. Resch-Genger, S. Lochbrunner, T. Opatz, K. Heinze, *ChemPhotoChem* **2017**, *1*, 344.
[53] S. M. Stevenson, M. P. Shores, E. M. Ferreira, *Angew. Chem. Int. Ed.* **2015**, *54*, 6506.
[54] F. J. Sarabia, E. M. Ferreira, *Org. Lett.* **2017**, *19*, 2865.
[55] T. H. Bürgin, F. Glaser, O. S. Wenger, *J. Am. Chem. Soc.* **2022**, *144*, 14181.
[56] S. Sittel, A. C. Sell, K. Hofmann, C. Wiedemann, J. P. Nau, C. Kerzig, G. Manolikakes, K. Heinze, *ChemCatChem* **2023**, *15*, e202201562.
[57] C. Wang, H. Li, T. H. Bürgin, O. S. Wenger, *Nat. Chem.* **2024**, *16*, 1151.
[58] R. F. Higgins, S. M. Fatur, S. G. Shepard, S. M. Stevenson, D. J. Boston, E. M. Ferreira, N. H. Damrauer, A. K. Rappé, M. P. Shores, *J. Am. Chem. Soc.* **2016**, *138*, 5451.

[59] F. J. Sarabia, Q. Li, E. M. Ferreira, *Angew. Chem. Int. Ed.* **2018**, *57*, 11015.
[60] Z. Shen, J.-L. Tu, *Eur. J. Org. Chem.* **2024**, e202401016.
[61] C. Förster, K. Heinze, *Chem. Soc. Rev.* **2020**, *49*, 1057.
[62] M. Dorn, N. R. East, C. Förster, W. R. Kitzmann, J. Moll, F. Reichenauer, T. Reuter, L. Stein, K. Heinze in *Comprehensive Inorganic Chemistry III*, Elsevier, **2023**, p. 707–788.
[63] F. Strieth-Kalthoff, M. J. James, M. Teders, L. Pitzer, F. Glorius, *Chem. Soc. Rev.* **2018**, *47*, 7190.
[64] S. Dutta, J. E. Erchinger, F. Strieth-Kalthoff, R. Kleinmans, F. Glorius, *Chem. Soc. Rev.* **2024**, *53*, 1068.
[65] M. DeRosa, *Coord. Chem. Rev.* **2002**, *233–234*, 351.
[66] P. Bayer, R. Pérez-Ruiz, A. Jacobi von Wangelin, *ChemPhotoChem* **2018**, *2*, 559.
[67] P. Bayer, J. Schachtner, M. Májek, A. Jacobi von Wangelin, *Org. Chem. Front.* **2019**, *6*, 2877.
[68] M. Prein, W. Adam, *Angew. Chem. Int. Ed.* **1996**, *35*, 477.
[69] C. K. Prier, D. A. Rankic, D. W. C. MacMillan, *Chem. Rev.* **2013**, *113*, 5322.
[70] S. Treiling, C. Wang, C. Förster, F. Reichenauer, J. Kalmbach, P. Boden, J. P. Harris, L. M. Carrella, E. Rentschler, U. Resch-Genger, C. Reber, M. Seitz, M. Gerhards, K. Heinze, *Angew. Chem. Int. Ed.* **2019**, *58*, 18075.
[71] P. Kusuma, P. M. Pattison, B. Bugbee, *Hortic. Res.* **2020**, *7*, 56.
[72] R. Bevernaegie, S. A. M. Wehlin, E. J. Piechota, M. Abraham, C. Philouze, G. J. Meyer, B. Elias, L. Troian-Gautier, *J. Am. Chem. Soc.* **2020**, *142*, 2732.
[73] S. D. A. Zondag, D. Mazzarella, T. Noël, *Annu. Rev. Chem. Biomol. Eng.* **2023**, *14*, 283.
[74] T. Noël, E. Zysman-Colman, *Chem. Catalysis* **2022**, *2*, 468.
[75] J. W. Tucker, Y. Zhang, T. F. Jamison, C. R. J. Stephenson, *Angew. Chem. Int. Ed.* **2012**, *51*, 4144.
[76] L. D. Elliott, J. P. Knowles, P. J. Koovits, K. G. Maskill, M. J. Ralph, G. Lejeune, L. J. Edwards, R. I. Robinson, I. R. Clemens, B. Cox, D. D. Pascoe, G. Koch, M. Eberle, M. B. Berry, K. I. Booker-Milburn, *Chem. Eur. J.* **2014**, *20*, 15226.
[77] T. H. Rehm, *Chem. Eur. J.* **2020**, *26*, 16952.
[78] M. Zhang, P. Roth, *Curr. Opin. Chem. Eng.* **2023**, *39*, 100897.
[79] A. Santoro, C. Sambiagio, P. C. McGowan, M. A. Halcrow, *Dalton Trans.* **2015**, *44*, 1060.
[80] E. A. Ünal, D. Wiedemann, J. Seiffert, J. P. Boyd, A. Grohmann, *Tetrahedron Lett.* **2012**, *53*, 54.
[81] K. Anandababu, R. Ramasubramanian, H. Wadepohl, P. Comba, N. Johnee Britto, M. Jaccob, R. Mayilmurugan, *Chem. Eur. J.* **2019**, *25*, 9540.
[82] A. M. McDaniel, H.-W. Tseng, N. H. Damrauer, M. P. Shores, *Inorg. Chem.* **2010**, *49*, 7981.
[83] S. Otto, M. Grabolle, C. Förster, C. Kreitner, U. Resch-Genger, K. Heinze, *Angew. Chem. Int. Ed.* **2015**, *54*, 11572.
[84] N. Sinha, J.-R. Jiménez, B. Pfund, A. Prescimone, C. Piguet, O. S. Wenger, *Angew. Chem. Int. Ed.* **2021**, *60*, 23722.
[85] J.-R. Jiménez, B. Doistau, C. M. Cruz, C. Besnard, J. M. Cuerva, A. G. Campaña, C. Piguet, *J. Am. Chem. Soc.* **2019**, *141*, 13244.
[86] R. D. Gillard, P. R. Mitchell, *J. Chem. Soc. A* **1968**, 2129.
[87] M. S. Baptista, J. Cadet, P. Di Mascio, A. A. Ghogare, A. Greer, M. R. Hamblin, C. Lorente, S. C. Nunez, M. S. Ribeiro, A. H. Thomas, M. Vignoni, T. M. Yoshimura, *Photochem. Photobiol.* **2017**, *93*, 912.
[88] H. H. Wasserman, J. L. Ives, *Tetrahedron* **1981**, *37*, 1825.
[89] W. Adam, A. Richter, J. Markus, *Acc. Chem. Res.* **1994**, *27*, 57.
[90] W. Adam, M. Braun, A. Griesbeck, V. Lucchini, E. Staab, B. Will, *J. Am. Chem. Soc.* **1989**, *111*, 203.
[91] E. D. Mihelich, D. J. Eickhoff, *J. Org. Chem.* **1983**, *48*, 4135.
[92] N. A. Porter, J. S. Wujek, *J. Org. Chem.* **1987**, *52*, 5085.
[93] M. S. Newman, H. A. Karnes, *J. Org. Chem.* **1966**, *31*, 3980.
[94] H. Kwart, E. R. Evans, *J. Org. Chem.* **1966**, *31*, 410.
[95] G. Lloyd-Jones, J. Moseley, J. Renny, *Synthesis* **2008**, *2008*, 661.
[96] T. Gendron, R. Pereira, H. Y. Abdi, T. H. Witney, E. Årstad, *Org. Lett.* **2020**, *22*, 274.
[97] S. K. Pedersen, A. Ulfkjær, M. N. Newman, S. Yogarasa, A. U. Petersen, T. I. Sølling, M. Pittelkow, *J. Org. Chem.* **2018**, *83*, 12000.
[98] A. F. Roesel, M. Ugandi, N. T. T. Huyen, M. Májek, T. Broese, M. Roemelt, R. Francke, *J. Org. Chem.* **2020**, *85*, 8029.
[99] P. Enders, K. Prane, E. Schönke, T. Taeufer, D. Michalik, J. Rabeah, R. Francke, *ChemCatChem* **2023**, *15*, e202300744.
[100] A. J. Perkowski, C. L. Cruz, D. A. Nicewicz, *J. Am. Chem. Soc.* **2015**, *137*, 15684.
[101] F. Glaser, O. S. Wenger, *Chem. Sci.* **2022**, *14*, 149.
[102] S. Lin, M. A. Ischay, C. G. Fry, T. P. Yoon, *J. Am. Chem. Soc.* **2011**, *133*, 19350.
[103] M. A. Cismesia, T. P. Yoon, *Chem. Sci.* **2015**, *6*, 5426.
[104] A. C. Sell, J. C. Wetzel, M. Schmitz, A. W. Maijenburg, G. Woltersdorf, R. Naumann, C. Kerzig, *Dalton Trans.* **2022**, *51*, 10799.
[105] D. Jespersen, B. Keen, J. I. Day, A. Singh, J. Briles, D. Mullins, J. D. Weaver, *Org. Process Res. Dev.* **2019**, *23*, 1087.
[106] B. Giese, J. A. González-Gómez, T. Witzel, *Angew. Chem. Int. Ed.* **1984**, *23*, 69.
[107] A. Borodine, *Justus Liebigs Ann. Chem.* **1861**, *119*, 121.
[108] L. McMurray, T. M. McGuire, R. L. Howells, *Synth.* **2020**, *52*, 1719.
[109] J. Schwarz, B. König, *Green Chem.* **2018**, *20*, 323.
[110] H. Roth, N. Romero, D. Nicewicz, *Synlett* **2016**, *27*, 714.

[111] B. Lantaño, A. Postigo, *Org. Biomol. Chem.* **2017**, *15*, 9954.
[112] G. Tarantino, C. Hammond, *ACS Catal.* **2018**, *8*, 10321.
[113] S. Ventre, F. R. Petronijevic, D. W. C. MacMillan, *J. Am. Chem. Soc.* **2015**, *137*, 5654.
[114] J. Xu, N. Liu, L. Zou, F. Cheng, X. Shen, T. Liu, H. Lv, R. Khan, B. Fan, *Asian J. Org. Chem.* **2019**, *8*, 261.
[115] D. D. M. Wayner, D. J. McPhee, D. Griller, *J. Am. Chem. Soc.* **1988**, *110*, 132.
[116] G. P. Girina, A. A. Fainzil'berg, L. G. Feoktistov, *Russ. J. Electrochem.* **2000**, *36*, 162.
[117] D.-M. Yan, Q.-Q. Zhao, L. Rao, J.-R. Chen, W.-J. Xiao, *Chem. Eur. J.* **2018**, *24*, 16895.
[118] F. J. Aguilar Troyano, K. Merkens, A. Gómez-Suárez, *Asian J. Org. Chem.* **2020**, *9*, 992.
[119] N. L. Reed, T. P. Yoon, *Chem. Soc. Rev.* **2021**, *50*, 2954.
[120] H. Guyon, H. Chachignon, D. Cahard, *Beilstein J. Org. Chem.* **2017**, *13*, 2764.
[121] Y. Qiu, A. Scheremetjew, L. H. Finger, L. Ackermann, *Chem. Eur. J.* **2020**, *26*, 3241.
[122] T. Koike, M. Akita, *Top. Catal.* **2014**, *57*, 967.
[123] D. A. Nagib, D. W. C. MacMillan, *Nature* **2011**, *480*, 224.
[124] I. Abdiaj, C. Bottecchia, J. Alcazar, T. Noël, *Synthesis* **2017**, *49*, 4978.
[125] S. Barata-Vallejo, B. Lantaño, A. Postigo, *Chem. Eur. J.* **2014**, *20*, 16806.
[126] K. R. Ryan, I. C. Plumb, *J. Phys. Chem.* **1982**, *86*, 4678.
[127] D. A. House, *Chem. Rev.* **1962**, *62*, 185.
[128] S. A. Shafiee, J. Aarons, H. H. Hamzah, *J. Electrochem. Soc.* **2018**, *165*, H785–H798.